

Mix-Crystallization of Two Dioxime Platinum Complexes by Coevaporation for Synthesizing One-Dimensional Superstructure

Kaoru Yamamoto,[†] Toshihide Kamata,^{*,‡} Yuji Yoshida,[‡] Kiyoshi Yase,[‡]
Toshio Fukaya,[‡] Fujio Mizukami,^{*,‡} and Toshiaki Ohta[†]

School of Science, The University of Tokyo, 7-3-1 Hongo, Bunkyo-ku, Tokyo 113-0033, Japan,
and National Institute of Materials and Chemical Research, 1-1 Higashi,
Tsukuba, Ibaraki 305-8565, Japan

Received November 7, 1997. Revised Manuscript Received March 17, 1998

Mixed crystals of the one-dimensional metal complexes, bis(dimethylglyoximato)platinum(II) and bis(diethylglyoximato)platinum(II), were synthesized by a coevaporation technique. The continuous energy shift of the $d-p$ transition was observed in the UV–vis absorption spectra of the coevaporated films. This energy shift shows that despite the difference in the crystal lattices between the two precursor complexes, both the metal complexes had mixed into the same column forming one-dimensional superstructures. Conventional X-ray diffraction and total reflection X-ray diffraction measurements showed that the anisotropic variation of the lattice constants depends on the mixing ratio. While the lattice constant parallel to the columns was approximately proportional to the mixing ratio, the variation of the constants perpendicular to the columns deviated substantially from a linear relation. This indicates that the one-dimensional framework of the mixed columns was maintained even though there is significant lattice mismatch between the precursor metal complexes.

Introduction

The organization of artificial superstructures has drawn lot of attention due to its ability to improve the physical properties of the original materials. A mixed crystal is one of the most typical forms of such superstructures, which often shows interesting physical properties¹ and crystal structures.² While a large number of studies on mixed crystals have been made for exclusively inorganic materials such as metals or semiconductors, the number of reports on mixed molecular crystals is limited.³ This is partly due to the difficulty in preparing the molecular crystal. On the other hand, recently, coevaporation has been applied to

fabricate various types of polymer films.^{4–6} In this technique, a copolymer film is fabricated by evaporating the precursors of the polymers from corresponding cells simultaneously in a vacuum chamber. We think that this technique is also advantageous for synthesizing mixed crystals of molecular compounds, since it is simple and requires no solvent.

In some dioximato complexes of d^8 -transition metal ions, the planar complexes stack face to face, forming a one-dimensional (1-D) metal chain.⁷ This leads to interesting electronic and optical properties.^{8–10} We have observed large optical nonlinearities for these materials that appear to result from the delocalized electronic states in the chain.¹¹ It is well-known that the third-order nonlinear optical property is enhanced when electron delocalization is confined to an appropriate low-dimensional space by organizing the structure

* To whom correspondence should be addressed.

[†] The University of Tokyo.

[‡] National Institute of Materials and Chemical Research.

(1) A characteristic electronic property of an inhomogeneous semiconductor is one of the most famous achievements of the study on the mixed crystal, which has given wide application in various fields of the electronics technology today. See for example: Burford, W. B.; Verner, H. G. *Semiconductor Junction and Devices*; McGraw-Hill: New York, 1965.

(2) For example, formation of a superlattice of zinc and copper is a well-known, interesting phenomena that resulted from synthesizing the mixed crystal. The superlattice is formed spontaneously by simply fusing and cooling the two metals. Kittel, C. *Introduction to solid state physics*; John Wiley & Sons: New York, 1986; Chapter 21.

(3) For instance, Engler et al. performed an investigation of the double phase transition of the charge-transfer salt of tetrafulvalene (TTF) with tetracyano-*p*-quinodimethane (TCNQ) by mixing heteromolecules into a TTF column. (a) Devreese, J. T.; Evrard, R. P.; van Doren, V. E. *Highly Conducting One-Dimensional Solids*; Plenum Press: New York, 1979; p 147. (b) Engler, E. M.; Scott, B. A.; Etemad, S.; Penney, T.; Patel, V. V. *J. Am. Chem. Soc.* **1977**, *99*, 5909.

(4) Salem, J. R.; Sequeda, F. O.; Duran, J.; Lee, W. Y.; Yang, R. M. *J. Vac. Sci. Technol. A* **1986**, *4*, 369.

(5) Ito, Y.; Hikita M.; Kimura T.; Mizutani T. *Jpn. J. Appl. Phys.* **1990**, *29*, 1128.

(6) Yoshimura, T.; Tatsuura, S.; Sotoyama, W. *Thin Solid Films* **1992**, *207*, 9.

(7) Endres, H.; Keller, H. J.; Lehmann, R.; Poveda, A.; Rupp, H. H.; van de Sand, H. *Z. Naturforsch.* **1977**, *32b*, 516.

(8) Belombé, M. M. *J. Solid State Chem.* **1977**, *22*, 151.

(9) Shirotani, I.; Kawamura, A.; Suzuki, K.; Utsumi, W.; Yagi, T. *Bull. Chem. Soc. Jpn.* **1991**, *64*, 1607.

(10) (a) Hara, Y.; Shirotani, I. *Solid State Commun.* **1976**, *19*, 171.

(b) Shirotani, I.; Onodera, A.; Hara, Y. *J. Solid State Chem.* **1981**, *40*, 180.

(11) (a) Kamata, T.; Fukaya, T.; Mizuno, M.; Matsuda, H.; Mizukami, F. *Chem. Phys. Lett.* **1994**, *221*, 194. (b) Kamata, T.; Fukaya, T.; Kodzasa, T.; Matsuda, H.; Mizukami, F.; Tachiya, M.; Ishikawa, R.; Uchida, T.; Yamazaki, Y. *Nonlinear Opt.* **1995**, *13*, 31.

of the material.¹²⁻¹⁴ The dioximato metal complexes originally form the 1-D electronic system delocalized along the metal chain. Thus, if heteromolecules can be inserted into the uniform molecular column, it should be possible to confine the delocalization into a nearly zero-dimensional space.

In this regard, features such as the nature of the metal ion, the ligands, the molecular arrangement, etc. in the hetero molecules are important. A portion of the metal ions of such a 1-D chain was substituted by other d^8 -transition metal ions in a previous paper.¹⁵ This proved to be effective in tuning the resonance energy that is related to the nonlinear optical property. However, this modification was not sufficient to induce a significant difference in the chemical and physical properties of the resultant materials.

Here, we direct our attention to controlling the distance between adjacent metals in the chain. The electron delocalization depends largely on the metal-metal distance.¹⁶ If the metal-metal distance in the uniform chain is extended at a site, the site will become an effective potential barrier. It is impossible to manipulate distances between the adjacent atoms for ordinary inorganic crystals of metals or semiconductors, because the superstructures will not be stable above a certain degree of lattice mismatch.¹⁷ Lattice mismatch can cause residual strain in the structure. Such a strain induced by the lattice mismatch, however, would be relaxed in the molecular crystals of the d^8 -transition metal dioximates, because of the weak packing forces of the organic ligands surrounding the central metal ion.^{18,19} This property will enable preparation of unique superstructures from metal complexes having different lattice constants.

In the present study, we have used two types of d^8 -transition metal dioximates with different metal-metal distances, bis(dimethylglyoximato)platinum(II) and bis(diethylglyoximato)platinum(II),^{20,21} and mix-crystallized them to synthesize 1-D superstructures by using coevaporation. The crystal structure of the coevaporated films was investigated through the variation of the delocalized electronic state in the UV-vis spectra. The vertical and in-plane structure of the mixed crystals in the film was analyzed by means of two kinds X-ray diffraction measurements, conventional $\theta-2\theta$ X-ray diffraction (XRD) and total reflection X-ray diffraction (TRXD).^{22,23} Comparing the two types of X-ray diffraction measurements, we investigated the detailed crystal

structure of the coevaporated films and discuss here the features of the columned structure.

Experimental Section

Two different kinds of metal complexes, bis(dimethylglyoximato)platinum(II) (**1**) and bis(diethylglyoximato)platinum(II) (**2**), were synthesized by mixing stoichiometric amounts of potassium tetrachloroplatinate(II) and the respective ligands, commercially available dimethylglyoxime and diethylglyoxime, in dimethylformamide solution. The diethylglyoxime for the above reaction was synthesized by the reaction of 3,4-hexanedione with hydroxylammonium sulfate in hot aqueous acetonitrile solution and purified by the recrystallization from ethanol solution. The thus obtained crude metal complexes were purified by repeated recrystallization from chloroform solution. The final products were washed with water and diethyl ether and dried in a vacuum desiccator for several days. All of the chemicals and solvents were reagent grade. The needle-shaped crystals of **1** were red-violet. Anal. Calcd for $C_8H_{14}N_4O_4Pt$: C, 22.59; H, 3.32; N, 13.18. Found: C, 22.73; H, 3.25; N, 12.83. The crystals of **2** were also needle-shaped and their color was yellow-brown. Anal. Calcd for $C_{12}H_{22}N_4O_4Pt$: C, 29.94; H, 4.61; N, 11.64. Found: C, 30.34; H, 4.62; N, 11.50.

Evaporated films of **1** and **2** and also coevaporated films were fabricated by means of an organic molecular beam deposition chamber²⁴ on fused silica substrates and Si(001) substrates at room temperature. The fused silica substrates were cleaned by ultrasonication in dilute NaOH solution and pure water after immersing them in 0.05 N NaOH solution overnight. The Si(001) substrates were used without further cleaning. The synthesized metal complexes were put into Knudsen cells and mounted in the deposition chamber. The pressure of residual gas was kept under 4×10^{-7} mbar in the chamber. The mixing ratio between the precursor complexes in the coevaporated film was controlled by varying the temperature of the cells; the range of temperature used was between 175 and 240 °C for **1**, and between 120 and 170 °C for **2**. The deposition rates were observed via a quartz crystal thickness monitor mounted in the deposition chamber. The total deposition rate was kept at ca. 3 nm/min. The thickness of the film was measured with a Tencor Alpha-step 300 surface profilometer after the fabrication. The final thickness of all the deposited films was approximately 100 nm. Fourier transform infrared (FT-IR) spectra have been measured using a Shimadzu FT-IR 8500 spectrometer to determine the mixing ratio of the precursor metal complexes in the coevaporated films. The mixing ratio was estimated by comparing the intensity of the characteristic absorption peak of each metal complex. The experimental error of the mixing ratio was confirmed to be less than 10%; the error was evaluated by comparing with standard samples prepared by mechanically mixing the two types of the metal complexes.

UV-vis absorption spectra were measured for the evaporated films on the quartz substrates as well as chloroform solutions of **1** and **2** by a Shimadzu UV-3100 spectrometer in a wavelength range between 200 and 900 nm. XRD patterns of the evaporated films on the quartz substrates were obtained with a Mac Science MXP-18 diffractometer with Cu-K α radiation (1.5405 Å). Reflections were recorded over a 2θ range from 5° to 50°. TRXD measurements were carried out for the evaporated films on the Si(001) substrates, which gave a high reflectance of incident X-rays due to its smooth surface with high electron density. The TRXD system used in this study was specially manufactured by Rigaku Co. Ltd. The sample film was mounted on a holder of an in-plane type goniometer (Rigaku Ultima). Incident white X-rays generated by a molybdenum target in a Rigaku RINT 2100 system

(12) Chemla, D. S.; Miller, D. A. B. *J. Opt. Soc. Am. B* **1985**, *2*, 1155.

(13) (a) Schmitt-Rink, S.; Chemla, D. S.; Miller, D. A. B. *Phys. Rev. B* **1985**, *32*, 6601. (b) Schmitt-Rink, S.; Miller, D. A. B.; Chemla, D. S. *Phys. Rev. B* **1987**, *35*, 8113.

(14) (a) Hanamura, E. *Phys. Rev. B* **1988**, *37*, 1273. (b) Hanamura, E. *Solid State Commun.* **1987**, *62*, 465.

(15) Kamata, T.; Fukaya, T.; Kodzasa, T.; Matsuda, H.; Mizukami, F. *Mol. Cryst. Liq. Cryst.* **1995**, *267*, 117.

(16) Banks, C. V.; Barnum, D. W. *J. Am. Chem. Soc.* **1958**, *80*, 4767.

(17) Matthews, J. W.; Blakeslee, A. E. *J. Cryst. Growth* **1974**, *27*, 118.

(18) So, F. F.; Forrest, S. R. *Phys. Rev. Lett.* **1991**, *66*, 2649.

(19) Koma, A.; Sunouchi, K.; Miyajima, T. *J. Vac. Sci. Technol. B* **1985**, *3*, 724.

(20) Hussain, M. S.; Salinas, B. E. V.; Schlemper, E. O. *Acta Crystallogr.* **1979**, *B35*, 628.

(21) Kamata, T.; Curran, S.; Roth, S.; Fukaya, T.; Matsuda, H.; Mizukami, F. *Synth. Met.* **1996**, *83*, 267.

(22) Marra, W. C.; Eisenberger, P.; Cho, A. Y. *J. Appl. Phys.* **1979**, *50*, 6927.

(23) Ishida, K.; Hayashi, K.; Yoshida, Y.; Horiuchi, T.; Matsushige, K. *J. Appl. Phys.* **1993**, *73*, 7338.

(24) Yoshida, Y.; Tanigaki, N.; Yase, K. *Thin Solid Films* **1996**, *80*, 281.

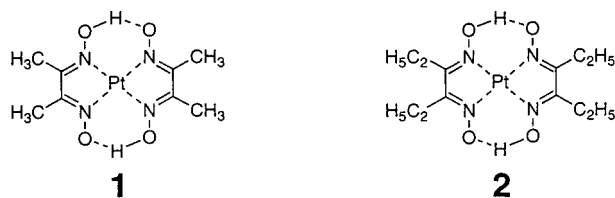


Figure 1. Molecular structures of bis(dimethylglyoximato)platinum(II) (**1**) and bis(diethylglyoximato)platinum(II) (**2**).

Table 1. Crystal Structures and Lattice Constants of Bis(dimethylglyoximato)platinum(II) (1**)²⁰ and Bis(diethylglyoximato)platinum(II) (**2**)²¹**

sample	1	2
crystal system	orthorhombic	monoclinic
space group	<i>Ibam</i>	<i>C2/m</i>
<i>a</i> (Å)	16.82	19.42
<i>b</i> (Å)	10.56	11.42 ($\beta = 91.6^\circ$)
<i>c</i> (Å)	6.51	3.55
<i>Z</i>	4	2
metal to metal distance (Å)	3.25	3.55

irradiated the sample film at a glancing angle of 0.2° , and the rays gave rise to total reflection at the boundary between the film and the substrate. An energy dispersive type of solid-state detector (Canberra GL0210R) which was fixed slightly away from the plane of an incident X-rays gave the diffraction profile as a function of the X-ray energy. This setup reduced background scattering from the substrates and thus made it possible to obtain the diffraction peaks of the in-plane structure of the film.^{22,23} The X-ray energy E_{hkl} , diffracted at the (*hkl*) plane, is expressed by

$$E_{hkl} = \frac{hcn}{2d_{hkl} \sin \theta} \quad (1)$$

where *h*, *c*, *n*, and d_{hkl} are Planck's constant, the velocity of light, the order of diffraction, and the lattice spacing of the (*hkl*) plane, respectively. The lattice spacing of the (*hkl*) plane was calculated by the formula together with the diffraction energy E_{hkl} and the Bragg angle θ . After each measurement, the θ value was calibrated by measuring the diffraction of KCl powder spread on the evaporated film.

Results and Discussion

Crystal Structures. Figure 1 shows the molecular structures of the metal complexes, bis(dimethylglyoximato)platinum(II) (**1**) and bis(diethylglyoximato)platinum(II) (**2**), used in this study. The crystal structures of **1** and **2**, which have been previously reported, are shown in Table 1.^{18,19} The crystals have a metal chain structure oriented along the crystal *c*-axis. The crystal of **1** is orthorhombic and has a metal–metal distance of 3.25 Å, whereas the crystal of **2** is monoclinic and has a metal–metal distance of 3.55 Å.

Endres et al. reported that the columned structures of d^8 -transition metal complex dioximates were dependent upon the (i) steric and (ii) electronic interactions between the adjacent complexes in the column.⁷ The steric factor is determined by the steric hindrance of the ligands, and the electronic factor is governed by the nature of the central metal ion and the electron density of the interacting *d* orbitals. In the present study, both metal complexes have similar alkyl substituent groups (CH₃, C₂H₅) on the dioximes which give almost the same electron-withdrawing abilities, and they have the same metal ion. Therefore, there is no substantial difference

in the electronic factor between the two types of the metal complexes. It is thought that the difference in the metal–metal distance between **1** and **2** depends on the steric hindrance of the alkyl substituent groups. The difference between the electronic states of the metal chain is attributed to the difference in the metal–metal distances in the chain.

UV–vis Spectrum. Figure 2 shows the UV–vis spectra of the evaporated films of **1** and **2**, with that of their chloroform solutions. In the spectrum of film of **1**, strong absorption bands appeared at wavelengths of 275, 328, and 681 nm. These three bands have been assigned to the π – π^* , metal to ligand charge transfer and *d*–*p* transitions, respectively.^{25,26} Similarly, the film of **2** showed the corresponding absorption bands at wavelengths of 279, 320, and 465 nm. It should be noted that in the absorption spectra of the complexes in the solution the *d*–*p* transition band is not observed, which clearly illustrates that intermolecular orbital interaction between the adjacent metal ions in the chain is present only in the crystal form.²⁷ The wavelengths of the absorption bands of the π – π^* and the metal to ligand charge-transfer transition were almost the same in both the spectra of **1** and **2**. This indicates the similarity of the intramolecular electronic states of the precursor metal complexes. On the other hand, the wavelengths of the *d*–*p* transitions were significantly different from each other; the wavelength of the transition of **2** is shorter than that of **1**. Since there is no substantial difference in the molecular electronic states of the precursor metal complexes, the difference in the *d*–*p* transitions is considered to originate from the difference in the metal–metal distance.

Figure 3 shows the UV–vis spectra of the coevaporated films prepared with various mixing ratios, as well as the respective films of the two types of the metal complexes. While the absorption bands of the π – π^* transition and the metal to ligand charge-transfer remained unchanged, the *d*–*p* transition band was broadened and shifted from the maximum wavelength of the absorption for **1** to **2**. If the two types of the metal complexes were crystallized independently in the coevaporated films, the two distinct *d*–*p* transition bands should appear in the coevaporated films. It is obvious, however, that the bands are not a simple overlap of the *d*–*p* transition bands of **1** and **2**. The energy shift of the *d*–*p* transition can be explained as the change of the electronic states caused by the formation of a mixed column. In the metal chain of the mixed column, the metal–metal distance will have a large value at the sites of **2** compared with others composed of **1**. This is because of the larger steric hindrance. Since there is no substantial difference in the intramolecular electronic states of the precursor metal complexes, the longer metal–metal site will have a substantial effect on the degree of the electronic delocalization.

The maximum wavelength of the *d*–*p* transition band is plotted as a function of the mixing ratio in Figure 4. A continuous shift of the *d*–*p* transition band is seen

(25) Ohashi, Y.; Hanazaki, I.; Nagakura, S. *Inorg. Chem.* **1970**, *9*, 2551.

(26) Zahner, J. C.; Drickamer, H. H. *J. Chem. Phys.* **1960**, *33*, 1625.

(27) Yamada, S. *Bull. Chem. Soc. Jpn.* **1951**, *24*, 125.

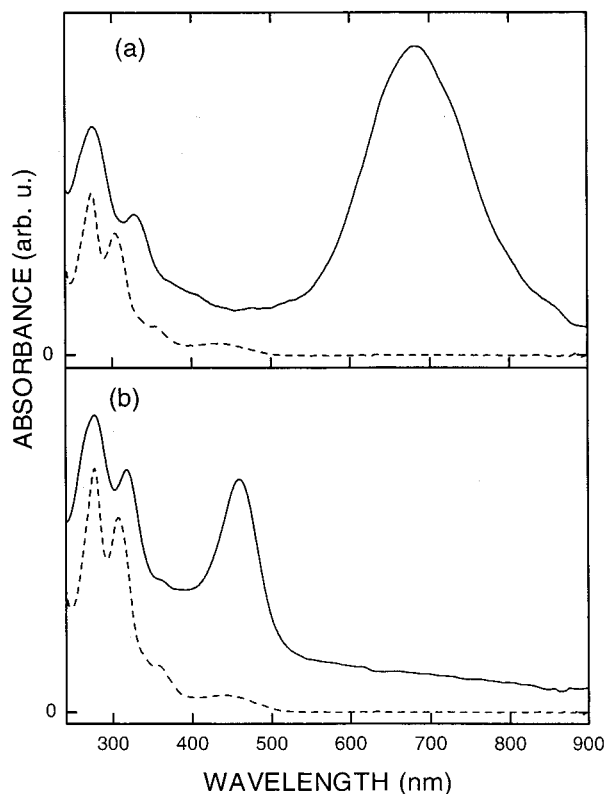


Figure 2. UV-vis spectra of the evaporated films of (a) **1** and (b) **2**, and of the chloroform solutions. Solid lines are of the films, and dotted lines of the chloroform solutions.

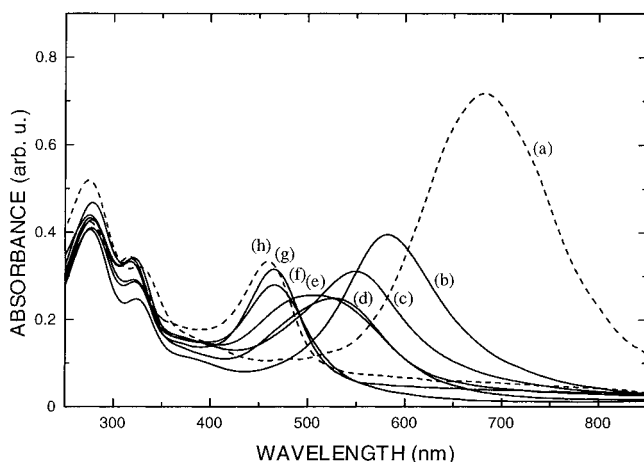


Figure 3. Dashed lines are UV-vis spectra of (a) **1** and (h) **2**, and solid lines b-g are those of the coevaporated films. The mixing ratios of **1** and **2** for b-g are 19:1, 17:8, 3:4, 5:8, 2:9, and 1:6, respectively. The absorbance is divided by the thickness of the films for normalization.

from the wavelength of **1** to that of **2**. This indicates that the two types of the metal complexes can be mixed in any ratio. A large variation can be seen in the slope at low fractions of **2**, and then the slope seems to tend to approach the wavelength of the *d-p* transition of **2**. This variation shows that the electron delocalization is deeply influenced by even a small amount of **2** mixed into the chain of **1**. This can be regarded as a barrier effect rather than the simple linear combination of molecular orbitals.

XRD. The XRD patterns of the films of **1** and **2** are shown in Figure 5, parts a and b. Sharp diffraction peaks appeared at $2\theta = 9.88, 19.82,$ and 29.94° for the

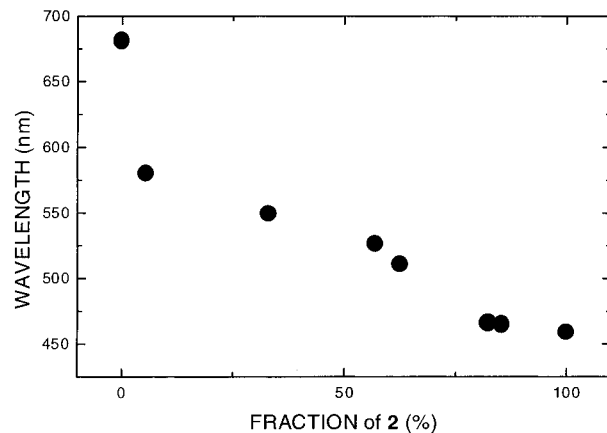


Figure 4. Peak wavelengths of the *d-p* transition band against the mixing ratio of **2** in the coevaporated films.

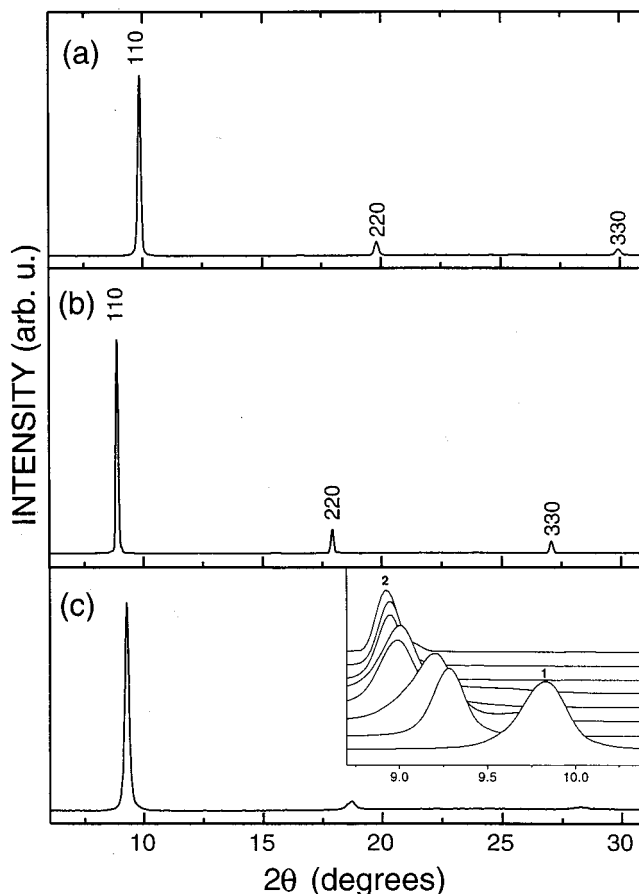


Figure 5. XRD patterns of evaporated films of (a) **1** and (b) **2**, and (c) the coevaporated film with a mixing ratio of **1:2** = 19:1. The inset in c shows diffraction peaks at around $2\theta = 9^\circ$ observed in the diffraction patterns of **1**, **2**, and the coevaporated films with various mixing ratios.

film of **1**, and at $8.90, 17.92,$ and 27.06° for the film of **2**. It was found from the lattice constants of the metal complexes that these three peaks correspond to the (110), (220), and (330) diffractions.^{18,19} The lattice spacing of (110) diffraction corresponds to the distance between adjacent columns. The appearance of these sharp (*nm*0) ($n = 1, 2, 3, \dots$) diffractions and the absence of the others indicate that the columns are well oriented and parallel to the substrate surface.

Figure 5c shows the XRD pattern of a coevaporated film with a mixing ratio of **1:2** = 19:1. Sharp (*nm*0)

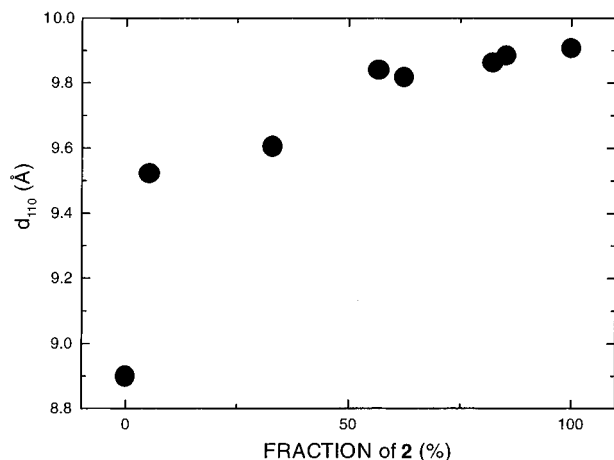


Figure 6. Lattice spacing of the (110) diffraction of the films of **1** and **2** and the coevaporated films against the **2** ratio.

diffraction peaks appeared at $2\theta = 9.28, 18.76,$ and 28.26° . If the two types of the metal complexes were crystallized independently in the film form, they should show a simple superposition of the X-ray profiles for the films of **1** and **2**.²⁶ However, in the diffraction profile of the mixed crystal, only one diffraction peak was observed between the ($nm0$) diffraction peaks of the precursor metal complexes. This indicates that the two types of the metal complexes form a mixed crystal in the coevaporated film. The high quality and uniformity of the mixed crystals is evidenced by the sharp diffraction peaks.

Figure 6 shows a correlation between the lattice spacing of the (110) planes and the mixing ratio of the mixed crystal. In general, the variation of the lattice spacing of mixed crystals will be directly proportional to the mixing ratio as predicted by Vegard's law.²⁹ However, the variation of the observed lattice spacing is not directly proportional to the mixing ratio. The lattice spacing tends to approach the spacing of **2** with the addition of a small amount of **2**. This discrepancy from Vegard's law can be attributed to the unique property of the column-structured crystals. We will later discuss the detailed structural properties of the mixed crystal after taking account of the characteristics of the molecular arrangement in the crystal.

TRXD. Since the column in the film was parallel to the substrate surface, only the arrangement of the columns in the crystal was determined by the XRD measurement. In this section, we investigate the molecular arrangement or the metal-metal distance in the column by means of TRXD measurements.

Si(001) was used as the substrate for the TRXD measurements to obtain a high reflectance of incident X-rays. It is known that the crystal structure of an evaporated film is strongly influenced by the substrate surface, which often results in the change of the crystal orientation or the structure of the deposited crystals.³⁰ In the present study, it was confirmed by XRD measurements that the crystal structure and the orienta-

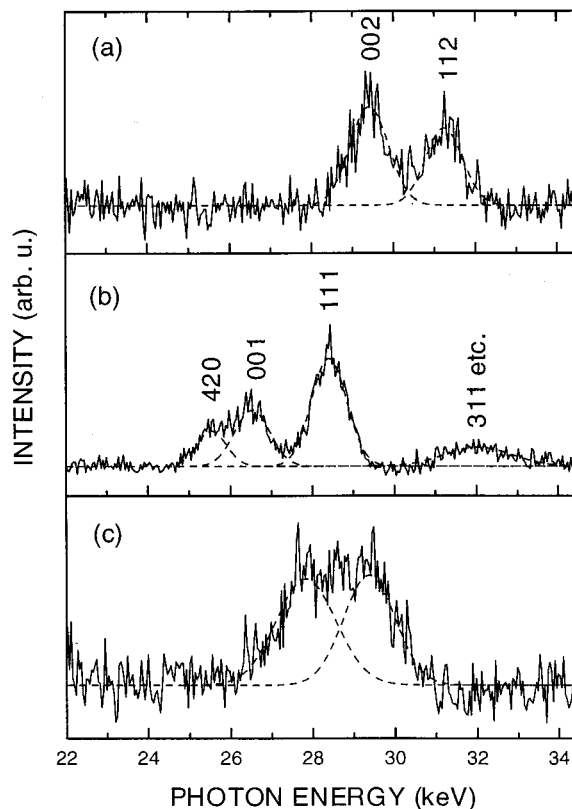


Figure 7. TRXD profiles of the evaporated films of (a) **1**, (b) **2**, and (c) their mixture with the mixing ratio of **1:2** = 17:8. The solid line is the experimental data, and the dashed line is the Gaussian fitted curve.

tions in the evaporated films on Si(001) are identical with those on a fused silica substrate.

Figure 7, parts a and b, show the TRXD profiles of the films of **1** and **2**. Diffraction peaks appeared at photon energies of 29.4 and 31.2 keV in the profile of the film of **1**. These peaks are ascribed to the (002) and (112) diffractions. In the TRXD profile of the film **2**, there appeared two major diffraction peaks and two weak peaks. The two major peaks at photon energies of 26.5 and 28.4 keV correspond to the (001), and a superposition of the (111) and the ($1\bar{1}\bar{1}$) diffractions of **2** correspond to the (002) and (112) diffractions of **1**. The weak peaks at 25.5 and around 32.0 keV are attributed to the (420) plane and a composite of the (311), ($3\bar{1}\bar{1}$), and (021) planes, respectively. The (001) diffraction of **2** and the (002) diffraction of **1** give the metal-metal distance.

Figure 7c shows the TRXD profile of a coevaporated film with a mixing ratio of **1:2** = 17:8. It was found that the profile of the coevaporated film is different from either of the TRXD profiles of the respective metal complexes. There is a broad peak between 26 and 31 keV in the profile. It should also be noted that the profile is different from the superposition of the profiles of the precursor metal complexes. This variation of the profile indicates, as proposed in the above discussion, a mixed crystal is formed in the coevaporated films.

A close analysis shows that the broad diffraction peak for the coevaporated film can be divided into two components of photon energy 27.9 and 29.4 keV. In the previous discussion, we have seen that both the UV-

(28) Hendricks, S. B.; Teller, E. *J. Chem. Phys.* **1942**, *10*, 147.

(29) (a) Vegard, L. *Z. Phys.* **1921**, *5*, 17. (b) Vegard, L. *Z. Phys.* **1921**, *5*, 393.

(30) Dann, A. J.; Hoshi, H.; Maruyama, Y. *J. Appl. Phys.* **1990**, *67*, 1371.

vis absorption and the XRD measurements for the coevaporated films showed a moderate change. The d - p absorption and the $(nm0)$ diffraction peaks varied continuously between the respective pure metal complexes with the mixing ratio. These results illustrate that the fundamental crystal structure of the mixed crystal is not varied substantially from those of the precursor metal complexes. Therefore, it is expected that the coevaporated film would give the same diffraction peaks to those of the precursor metal complexes. From the fact that the films of the precursor metal complexes gave the two major diffraction peaks, $(00a)$ and $(11a)$ ($a = 1$ or 2), the two broad peaks that appeared in the coevaporated film should also be attributed to these peaks. The value of a indicates different space groups depending on whether the molecular stacking in the column involves a rotation of 90° (the column of **1**), or not (the column of **2**). It is considered that the two broad peaks at 27.9 and 29.4 keV correspond to $(00a)$ and $(11a)$ respectively, since the diffraction peaks of a mixed crystal are situated between the peaks observed for the constituents. The space group of the mixed crystal remains uncertain, but the averaged metal-metal distance was calculated from the energy of the $(00a)$ diffraction, to be 3.39 Å.

Structural Analysis of the Mixed Crystal. On the basis of the result of TRXD and XRD measurements, here we discuss the three-dimensional characteristics of the molecular arrangement in the mixed column, also the reason why the precursor metal complexes were able to be mixed into the same column structure despite the large difference in the lattice constants.

Supposing that the variation of averaged lattice spacing of the mixed crystal follows Vegard's law, the lattice spacing can be estimated by

$$d_{\text{mix}} = d_1 + (d_2 - d_1) \times x_2 \quad (2)$$

In the formula, d_{mix} denotes the lattice spacing of certain planes of the mixed crystal. Here, we would like to investigate the $(00a)$ and (110) planes, which were measured by XRD and TRXD measurements, respectively. Similarly, d_1 and d_2 are the lattice spacings of the corresponding lattice planes of **1** and **2**. The value of x_2 indicates the proportion of **2** in the mixed crystal.

By eq 2, the averaged lattice spacing of the $(00a)$ and (110) planes in the mixed crystal with a ratio of **1:2** = 17:8 was calculated to be 3.35 ± 0.03 and 9.24 ± 0.09 Å, respectively. Here, the margin of the error was calculated by taking account of the error of the mixing ratio of the two precursor complexes estimated by the FT-IR measurements. The calculated lattice spacing of the $(00a)$ planes, 3.35 ± 0.03 Å, which indicates the metal-metal distance, was found to correspond to the results obtained from TRXD measurements of 3.39 Å. It is thought that the variation of the metal-metal distance of the mixed crystal was approximately proportional to the mixing ratio. This indicates that the two types of the metal complexes were closely packed in the column, and thus the distance between the molecules in the column was governed by the charac-

teristic distance of the respective molecules. On the other hand, the calculated lattice spacing of the (110) planes by eq 2, 9.24 ± 0.09 Å, which denotes the distance between the columns, was far from the experimental value of 9.59 Å observed by XRD. It was noted earlier that the distance between the columns of the mixed crystal tends to approach that of **2** even with a small addition of **2** in **1**. Hence, the columns seem to be loosely packed in the mixed crystal.

It was found that there is substantial difference in the mixing ratio dependence of the variation of the lattice spacings between planes parallel and perpendicular to the column. This difference is thought to depend on the one-dimensionality of the columned structure. The planar metal complexes are tightly stacked on the top of each other in the column structure by a strong attractive force. The origin of this force is partly in the dispersion force between the wide molecular surfaces and also in the metal-metal interactions between the adjacent molecules. On the contrary, the packing force between the columns will be weak, because the metal complexes are surrounded by the hydrogens of the alkyl substituent groups. The one-dimensional framework of the column was retained mainly because of the large difference in the interaction within and between the mixed columns. It is also possible that the larger ligands of **2** chiefly interfered with the adjacent columns, which might have resulted in the deviation of the lattice constants from Vegard's law only in the direction perpendicular to the columns.

Conclusion

This paper presented a study on the preparation of mixed molecular crystals by coevaporation and proposed a new way of fabricating 1-D superstructures.

From the UV-vis measurements it has been shown that it is possible to mix two precursor metal complexes into the same columned structure by coevaporation. The large energy shift of the d - p absorption due to a small addition of **2** into **1** indicates that the enlarged portion in the mixed metal chain influenced the 1-D electronic system as effective potential barriers. The three-dimensional structure of the mixed crystal was investigated by comparing the results of two types of X-ray diffraction measurements, namely XRD and TRXD. The two diffraction measurements revealed that there is large difference in the mixing ratio dependence between the lattice constants parallel and perpendicular to the columns. While the variation of the lattice constant parallel to the columns was approximately proportional to the mixing ratio, the variation perpendicular to the columns was appreciably deviated from the linear proportion. This anisotropic variation of the lattice constants originated in the rigid columned structure; while the packing force between the columns was weak, the molecules were closely packed in the columns to form a rigid 1-D framework.

The formation of such a rigid columned structure is advantageous to develop artificial superstructures with low dimensionality. It was found that we could vary a part of the metal-metal distance in the metal chain by introducing a hetero type of metal complex. Because the one-dimensionality of the metal chain is maintained

in good condition by the rigid column formation, we can suppress defects resulting from the introduction of the heteromolecule in the electronic system. Furthermore, it is also possible to exchange a part of the metal ions in the column, which have been demonstrated in the previous paper. Combining these structural organizations, we expect to be able to fabricate various new superstructures unique to molecular crystals and develop artificial low-dimensional electronic systems.

Acknowledgment. The authors are grateful to Takeshi Hanada in National Institute of Materials and Chemical Research for useful discussions on the X-ray diffraction of the mixed crystal. K. Yamamoto is deeply grateful to Padmakumar Nair and Mitsuhiro Kanakubo in National Institute of Materials for helpful advices and correction of English.

CM9707317